Identifying periods of clear sky direct normal irradiance

Larrañeta, M.[1], Reno, M. J.[2], Lillo-Bravo, I.[3], Silva-Pérez, M.A.[3]

[1] Andalusian Association for Research and Industrial Cooperation (AICIA).

[2] Sandia National Laboratories.

[3] Department of Energy Engineering, University of Seville.

Corresponding author:

Miguel Larrañeta, Andalusian Association for Research and Industrial Cooperation, Camino de los Descubrimientos s/n. 41092, Seville, Spain.

Phone/Fax number: (+34)954487237/ (+34)954487233

E-mail: mlarraneta@gter.es

Abstract

When modeling the effect of the cloud transients in the Direct Normal Insolation (DNI), it is particularly relevant to identify those moments in which there are no clouds between the observer and the sun. In this paper, we present a simple algorithm for offline detection of situations where the sun path to the observer is not obstructed by any cloud. The algorithm is based on the characterization of the relations between the measured and the clear sky curves. The clear sky identification module consists of three evaluation and detection metrics: hourly mean, slope, and line length criterion. All of them rely on the assessment of the measured data against the clear sky generated data. The conjunction of the fulfillment of the three criteria leads to the clear sky hour identification. We validate our algorithm by comparing our results with those obtained from a recently published clear sky detection algorithm that uses high temporal resolution Global Horizontal Irradiation (GHI) as the input. We obtain a 98% agreement when having more than 50 minutes identified as clear.

Keywords

DNI; clear sky; solar radiation models

1 Introduction

There are several alternatives when defining the clear sky condition and the clear sky irradiance [1]. The most common definition is the absence of visible clouds across the entire sky dome and the irradiance occurring these conditions is the clear sky irradiance. In Concentrated Solar Power (CSP) systems it is also interesting to identify periods where there are no visible clouds between the observer (solar field) and the sun although there may be clouds in the rest of the sky dome since DNI is not affected by diffuse radiation scattered by the clouds and plant production will be similar than under clear sky conditions. We use the term "clear sky equivalent DNI" to refer to either DNI during clear sky conditions or DNI during all-sky conditions that is similar to clear sky irradiance. This paper is valuable to identify both clear sky periods and periods with irradiance similar to clear sky irradiance relying on hourly DNI data.

In an automated performance evaluation of a CSP system, the determination of periods with irradiance similar to clear sky irradiance would result of great interest for the detection of system degradations and faults.

Many clear sky detection methods rely on measured irradiance, mainly in GHI and Diffuse Horizontal Irradiation (DHI) of high temporal resolution [1] but only few use DNI measurements and none of them in an hourly time step. Perez et al. [2] proposed a formulation of sky clearness ε using the diffuse irradiance and beam irradiance. Reno et al. [3] developed an endogenous statistical model for GHI observations. This method uses five criteria to compare a 10-min sliding window containing ten observations to a corresponding clear sky model for the same period. Each 1-min measurement is classified as clear only if threshold values for all five of the clear-sky criteria are met. Inman et al. [4] applied the same methodology for DNI time series. In this case, the thresholds for DNI were slightly relaxed because of the increased variability in the observational DNI time series. Nou et al. [5, 6] applied a multi-resolution analysis based on the discrete wavelet transform for the same purpose using also 1-min data. The signal was decomposed into approximations and details through Low-Pass and High-Pass filters highlighting significant changes in DNI related to the presence of clouds.

High temporal resolution DNI series are needed for the design and evaluation of CSP plants. Due to the relative difficulty of having extensive time series, these are in some cases, synthetically generated. When modeling high temporal resolution DNI data, it is particularly relevant to identify periods with irradiance similar to the clear sky irradiance to decide if disturbances in the solar radiation should be generated [7] especially in hazy days when the DNI may show negligible fluctuations [8].

To distinguishing clear sky periods, some authors have also classified cloud types using measured radiation data combined with other devices. In the recent years, cloud cover and types have been generally addressed using sky imagers. Martínez-Chico et al. [9] defined the sky condition by means of the levels of attenuation of the DNI reaching the earth surface. The most representative characteristics the type of cloud producing each sky condition were described using a total sky imager. Other measurements like illuminance scan data [10], ground-based radar data [11], Lidar backscatter measurements [12], longwave downwelling radiation along with shortwave downwelling radiation [13] or with other meteorological parameters [14] have been also used in cloud type detection.

In this paper, we present a methodology for the identification of periods with clear sky equivalent DNI only from hourly DNI data, without the necessity of using other devices. The approach is performed comparing the differences between the means, the slopes and the lengths of the measured and theoretical clear sky curves. For this purpose, an empirical clear sky fit has been performed. The algorithm is not sensitive to the choice of the clear sky model because we have implemented an iterative adaptive method; nevertheless, the methodology relies on the proper fit of the clear sky model. The performance of the model has been addressed comparing the results with a recently published algorithm showing satisfactory results besides having a simpler structure.

2 Clear sky fit

The algorithm proposed in this paper is strongly dependent on the clear sky model fit. In this sense, two handicaps are found; the clear sky definition and the limitation on the use of only hourly DNI data.

The clear sky definition involves identifying periods with high clouds or cirrus as non-clear sky instants while the instantaneous radiation fairly reflect fluctuations from the clear sky shape. Because this work is intended to be an intermediate block when generating high temporal resolution synthetic irradiance data, identifying those moments as non-clear would lead to the generation of unreal fluctuations.

The selected clear sky model requires an empirical adjustment to the clear sky DNI that in this case is only hourly data. In the implementation of this methodology, some of the generated clear sky data overcome the physical limits due to the shortage of hours per day that can be used to fit the model. In the analyzed latitude, daylight hours vary from 9-15, including hours with low solar elevations.

The first handicap is assumed the main source of error in the methodology while the second is solved by imposing extreme values in the parameters that define the clear sky profiles calculated from the analysis of the behavior of these parameters on the same site for a period of 14 years.

In the present methodology any of the well-known DNI clear sky models [15] could be used, based on the available information. Here in this case, we use the clear sky model A-B Proposed by Silva-Perez [16]

$$I_{bn_{cs}} = I_{cs} \cdot E_0 \cdot \frac{A}{1+B \cdot m_R} \quad (1)$$

Where m_R is the relative air mass determined according to the expression of Kasten and Young, [17] I_{cs} is the solar constant, E_0 the correction due to Earth-Sun distance and A and B are empirical parameters intended to model the state of transparency or turbidity of the atmosphere. This model is a modification of the kastov´s formula quoted, among others, by Kondayev [18]:

$$I_{bn_{cs}} = I_{cs} \cdot E_0 \cdot \frac{1}{1+c \cdot m_R} \quad (2)$$

The introduction of the second parameter is justified by the fact that, as noted by Murk [19], at least two parameters are required to model the time evolution of the solar irradiance. This results from the effect described by the Scottish physicist James David Forbes, known as virtual diurnal variation: the transparency of the atmosphere depends on the solar height nonlinearly, even in the case of a stationary atmosphere and azimuthally homogeneous, because when passing through a large air mass, the radiation in wavelengths with higher monochromatic extinction coefficients expires before, remaining mainly components with lower monochromatic extinction coefficients.

The parameter A mainly realizes the processes of absorption in certain spectral bands, particularly those in which the absorption is stronger, while B realizes primarily scattering phenomena, but also of weak absorption phenomena. In any case, A and B are not independent. Consider that certain elements (including aerosols) play an important role in both processes of dispersion and the absorption; therefore, their presence in the atmosphere will be reflected in both parameters.

Water vapor and atmospheric aerosols are predominant components in the absorption processes. Regarding dispersion processes, aerosols play an imperative role. Furthermore, the presence of these two components in the atmosphere is quite variable. According to the above reasoning, the presence of water vapor will be reflected mainly in the parameter A, which will be lower the greater the presence of water vapor in the atmosphere, and the presence of aerosols is mainly reflected in the B parameter, whose value will be greater the higher content of aerosols.

In a first approach, intending to have an initial envelope clear sky curve, we use the parameters A and B fitted to the maximum irradiance values divided by the correction due to Earth-Sun distance obtained for each solar angle higher than 5°. The hourly direct fraction index k_b^h [20] is afterwards calculated as:

$$k_b{}^h = I_{bn}{}^h / I_{bn_{cs}}{}^h \tag{3}$$

Where, $I_{bn}{}^h$ is the observed hourly average direct normal irradiance and $I_{bn_{cs}}{}^h$ is the hourly average clear-sky DNI. The initial clear sky hours are defined as hours whose k_b^h is higher than 0.65.

The process continues with the analysis of the initial number of clear sky hours for each day. If it is higher than two hours, we run the empirical fit again but in this time, matching it to the points identified as initial clear sky hours and using a least squares procedure. Under the assumption that the state of the atmosphere does not change substantially from one day to the next, the fitted A and B parameters will remain constant until the exposed conditions appear again. As explained before, the posed conditions may not entail a proper fit, therefore if the fitted A and B parameters reach a threshold maximum and minimum value, they will remain constant from the previous day.

Those threshold maximum and minimum values are calculated from an extensive database. In this case, we use measurements of direct solar radiation during 14 years (2000–2013) for the location of Seville. The measurements were taken with a sampling and storing frequency of 0.2 Hz. A first class Eppley NIP pyrheliometer coupled to a sun tracker Kipp&Zonen 2AP measured the DNI. The devices are located at the meteorological station of the Group of Thermodynamics and Renewable Energy of the University of Seville. We calculate the A and B parameters assuming the same conditions as exposed in the previous paragraph, but in this case, due to the high resolution of the available data, three hours of clear hours corresponds to much more points and therefore, the fit is generally more concrete. The threshold maximum and minimum values are the Percentile 99 and Percentile 01 of the obtained A and B values for the entire dataset. Figure 1 represents the boxplot of the A and B values calculated for 14 years at the location of Seville.

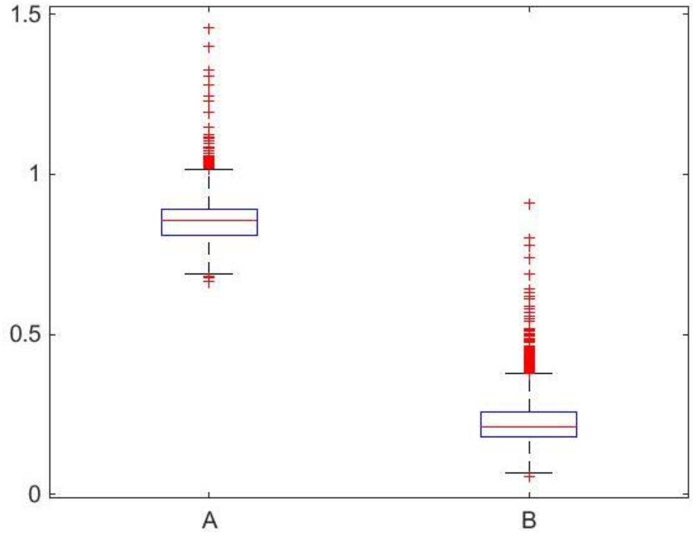

Fig 1. A-B clear sky model parameters boxplot for 14 years at the location of Seville.

In order to appreciate the strength of correlation between both parameters we present a scatter plot of the daily fitted values in figure 2. Outliers have not been included in the plot

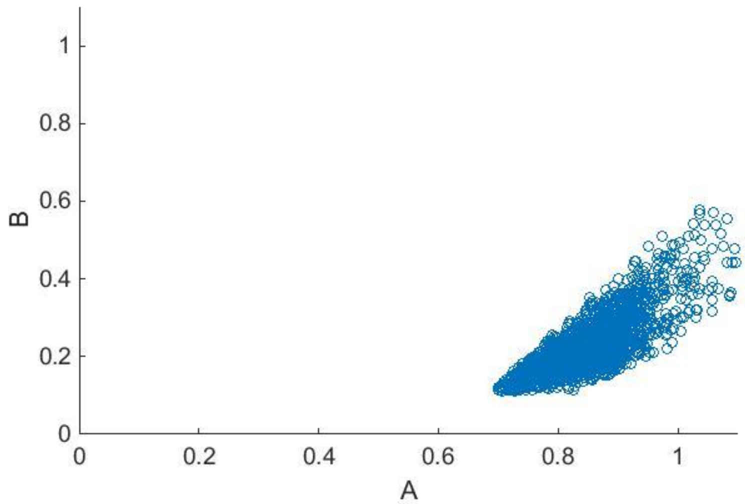

Fig 2. A-B clear sky model parameters scatter plot for 14 years at the location of Seville.

3 Clear sky identification

Once obtained a clear sky curve fitted to each day, the next step consists of identifying periods with irradiance similar to the clear sky irradiance from the comparison of both curves hour by hour. The criteria used are based on [3] but because of the lower resolution data, we use only 3 of the 5 metrics originally proposed. Each hour is defined by two points, which leads to the comparison of linear segments. In clear conditions, at lower solar angles the variation of the hourly mean from one hour to the next is greater than for solar angles close the solar noon because the daily clear sky solar radiation curve is similar to a Gaussian curve. Therefore, we divide the daily curves into three intervals, each space covers 1/3 of the maximum solar angle. Figure 2 presents an example of the threshold values for each interval on the clear sky curve of a summer day.

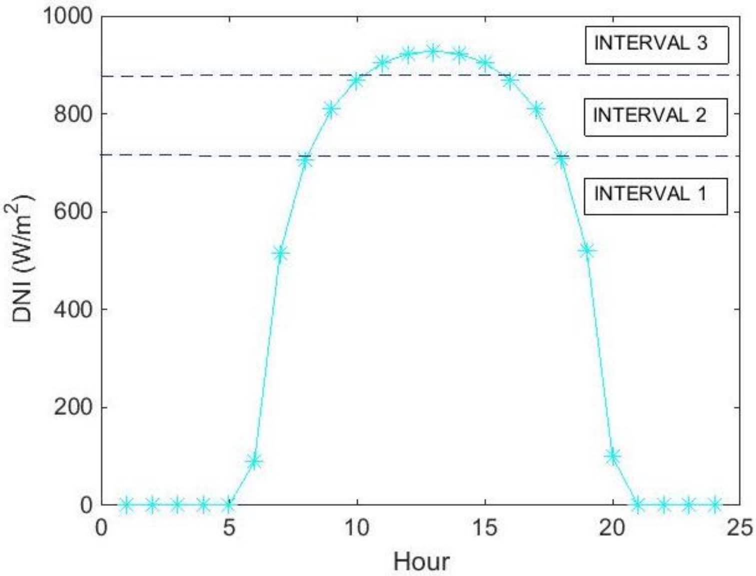

Fig 3. Example of the three independently analyzed intervals depending on the maximum solar elevation for a summer day.

The identification of clear sky equivalent DNI consists on the concurrence of three criterion depending on the hourly mean and the slope and length of the straight line. Note that each criterion is not overly restrictive on its own, but the combination of the three of them would determine whether the analyzed hour is clear or not.

3.1 Hourly mean criterion

The first criterion involves the comparison of the hourly clear sky and measured means. The analysis consist in the calculation of the absolute percentage differences of the measured and clear sky radiation D_{cs-m}^{i}:

$$D_{cs-m}^{i} = \text{abs}\left(100 \cdot \frac{I_{bn_{cs}}^{i} - I_{bn}^{i}}{I_{bn}^{i}}\right) \quad (4)$$

Whenever D_{cs-m}^{i} is lower than 2.5%, the hour is classified as clear regardless the rest criteria output. This statement includes points where the measured DNI is higher than the clear sky DNI. Table 1 presents the limit values for each solar interval.

Table 1. Threshold clear sky identification values for the hourly mean criterion

Solar elevation	***Condition***	***Classification***
Interval 1	$D_{cs-m}^{i} < 35\%$	Clear
Interval 2	$D_{cs-m}^{i} < 15\%$	Clear
Interval 3	$D_{cs-m}^{i} < 10\%$	Clear

The shadows that come from the horizon obstacles and the fact of working with hourly means that carries a source of error, affect mainly low solar elevations (interval1). For these reasons, the threshold clear sky identification values in this criterion are less restrictive the lower the solar angle. The threshold $D_{cs\text{-}m}{}^{i}$ values correspond to quantiles of about 0.5 (0.46, 0.54 and 0.52 for the intervals 1, 2 and 3 respectively). Values adjusted to the location under study.

3.2 Slope criterion

The second step consists on the comparison of the slopes of the straight lines that joins two hourly mean values. For each hour, the slope would be the variation of the hourly DNI divided by the variation of time.

$$S_{cs}{}^{i} = {I_{bn_{cs}}{}^{i} - I_{bn_{cs}}{}^{i-1}} \Big/ {T^{i} - T^{i-1}} \tag{5}$$

$$S_{m}{}^{i} = {I_{bn}{}^{i} - I_{bn}{}^{i-1}} \Big/ {T^{i} - T^{i-1}} \tag{6}$$

Where the subscript *i* represents the time instant, *cs* the clear sky and *m* the measured data.

We assume that a different measured and clear sky slope sign involves an alteration on the sky condition caused to passing clouds. The condition for the clear sky identification in this criterion is expressed in Table 2.

Table 2. Condition for the clear sky identification for the slope criterion.

Solar elevation	***Condition***	***Classification***
Interval 1,2,3	Sign ($S_{cs}{}^{i}$) = Sign ($S_{m}{}^{i}$)	Clear

3.3 Line length criterion

The third step consist on the analysis of the length of the straight lines that joins two hourly mean values and their corresponding absolute percentage differences calculated as follows:

$$L_{cs}{}^{i} = \sqrt{(I_{bn_{cs}}{}^{i} - I_{bn_{cs}}{}^{i-1})^2 + (T^{i} - T^{i-1})^2} \tag{7}$$

$$L_{m}{}^{i} = \sqrt{(I_{bn}{}^{i} - I_{bn}{}^{i-1})^2 + (T^{i} - T^{i-1})^2} \tag{8}$$

$$LD_{cs-m}{}^{i} = \text{abs}\left(100 \cdot \frac{L_{cs}{}^{i} - L_{bn}{}^{i}}{\mathrm{L}_{bn}{}^{i}}\right) \tag{9}$$

Following a similar assumption as in the slope criterion, a great difference in the line length longitude represents an alteration condition due to passing clouds. The line length that joins two hourly mean clear sky values varies substantively depending on the solar elevation therefore we combine the absolute differences on the line lengths and the clear sky line length. The combination of these calculations leads to the line length clear classification as presented in Table 3.

Table 3. Line length classification conditions for the clear sky identification.

Solar elevation	***Condition***	***Classification***
Interval 1	$LD_{cs\text{-}m}^{i}$ < 25 % & L_{cs}^{i} > 220	Clear
Interval 2	$LD_{cs\text{-}m}^{i}$ < 35 % & L_{cs}^{i} > 110	Clear
Interval 3	$LD_{cs\text{-}m}^{i}$ < 120 % & L_{cs}^{i} < 30	Clear

For low solar angles, the absolute percentage condition is lower than for high solar angles however, the line lengths follow the inverse pattern. The threshold $LD_{cs\text{-}m}^{i}$ values correspond to quantiles of 0.46, 0.54 and 0.52 for the intervals 1, 2 and 3 respectively.

4 Iterative process

Once identified the periods with irradiance similar to the clear sky irradiance, we execute a daily iterative process that consists on the readjustment of the clear sky model to those periods through the process exposed in paragraph 2 until the A and B parameters converge. Figure 3 shows the block diagram of the process. The subscript *j* represents the modeled day

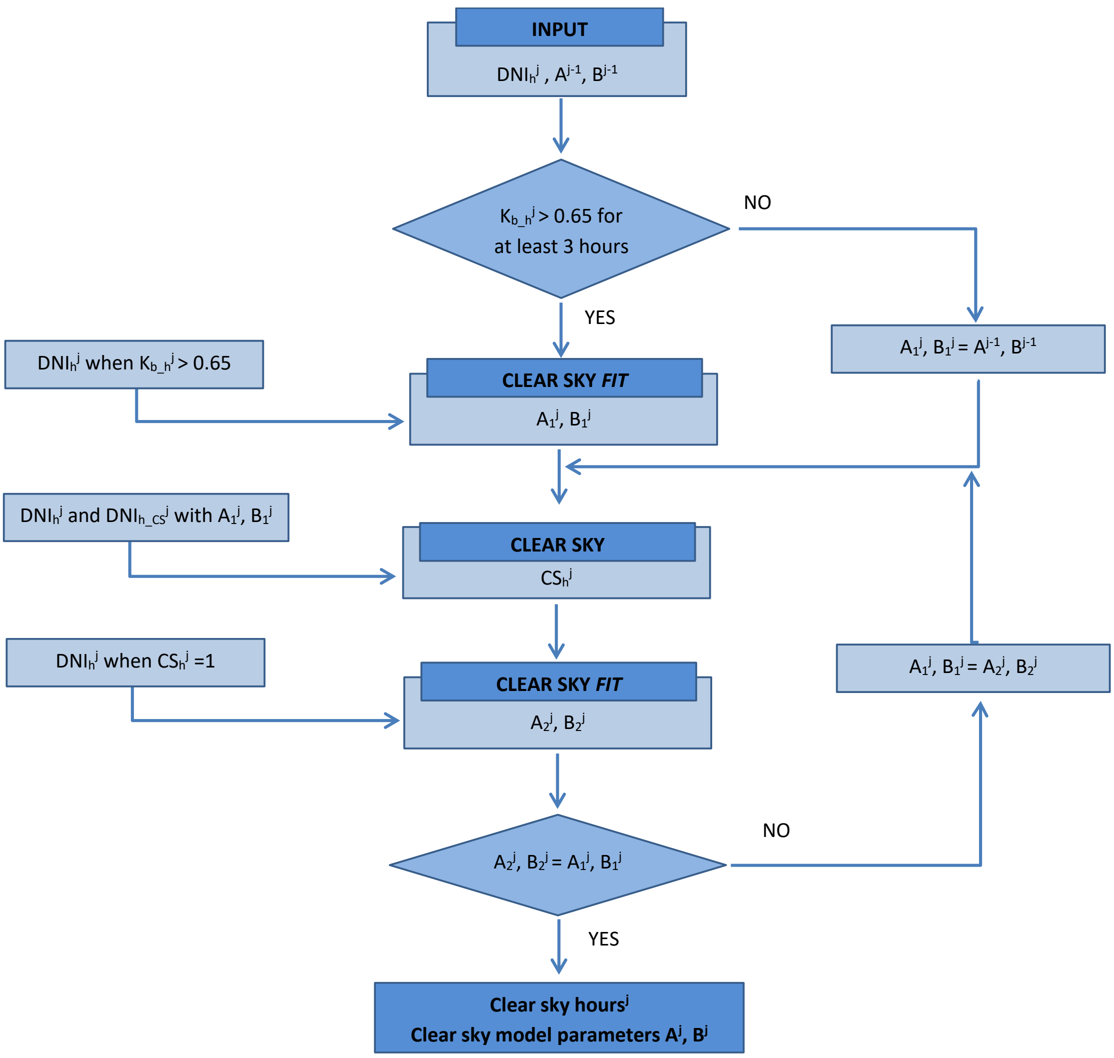

Fig 4. Block diagram of the process

5 Results

To assess the performance of the model, we have utilized one year (2014) of measurements of DNI and GHI reregistered with a sampling and storing frequency of 0.2 Hz at the meteorological station of the Group of Thermodynamics and Renewable Energy of the University of Seville with a secondary standard Kipp&Zonen CMP21 and a first class Eppley NIP pyrheliometer coupled to a sun tracker Kipp&Zonen 2AP. The instantaneous DNI data has been integrated into hourly means for the execution of the model and to 10-min resolution to observe the performance of the model. Ten consecutive daily profiles are illustrated in Figure 4. The left figures show the DNI hourly means of the daily profiles and the figures on the right show the daily profiles in 10-min means. The measured data is printed in discontinuous blue, the identified clear sky equivalent DNI periods are presented in continuous black and for the case of hourly means and the clear sky fitted shape is presented in a doted cyan line.

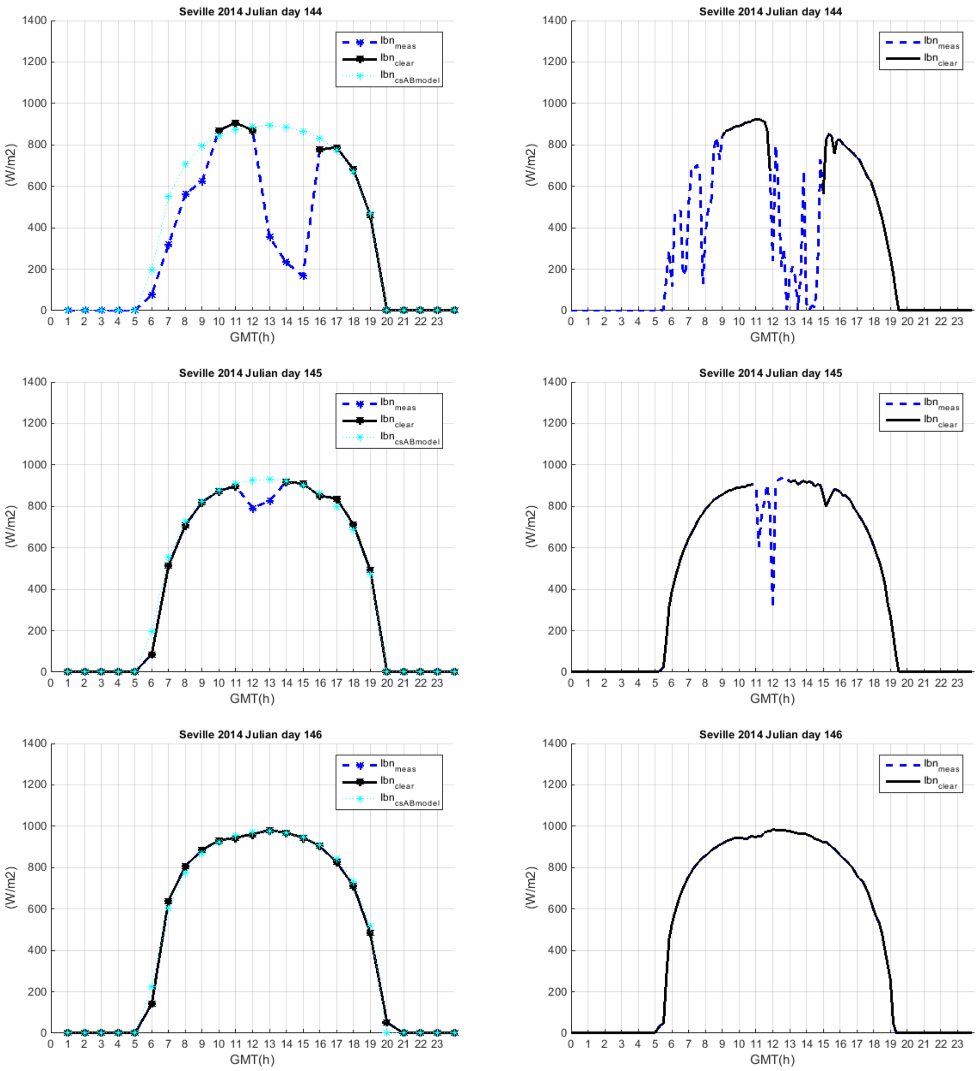

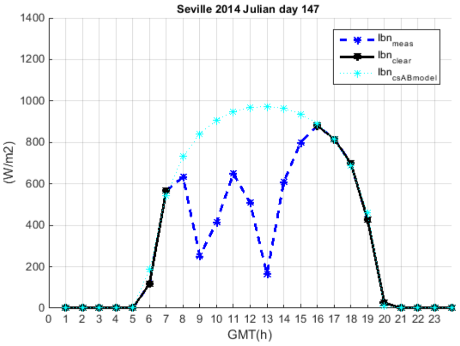
Seville 2014 Julian day 147
Ibn_{meas}
Ibn_{clear}
$Ibn_{csABmodel}$
(W/m2)
GMT(h)
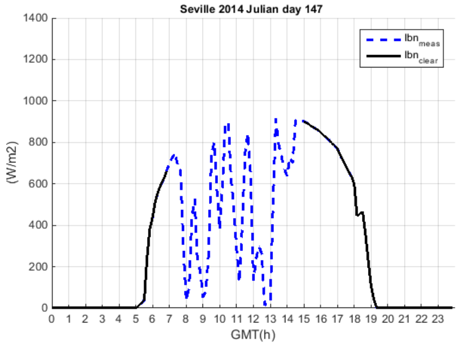
Seville 2014 Julian day 147
Ibn_{meas}
Ibn_{clear}
(W/m2)
GMT(h)
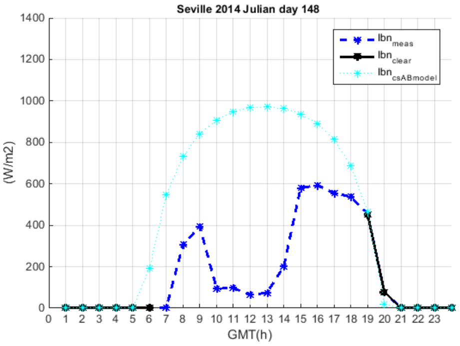
Seville 2014 Julian day 148
Ibn_{meas}
Ibn_{clear}
$Ibn_{csABmodel}$
(W/m2)
GMT(h)
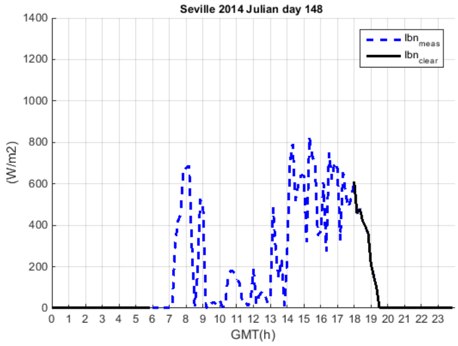
Seville 2014 Julian day 148
Ibn_{meas}
Ibn_{clear}
(W/m2)
GMT(h)
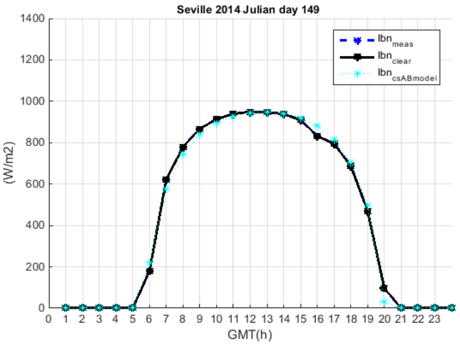
Seville 2014 Julian day 149
Ibn_{meas}
Ibn_{clear}
$Ibn_{csABmodel}$
(W/m2)
GMT(h)
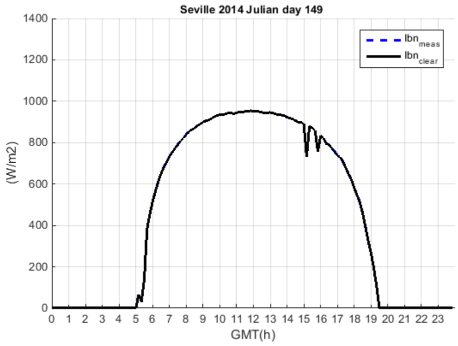
Seville 2014 Julian day 149
Ibn_{meas}
Ibn_{clear}
(W/m2)
GMT(h)
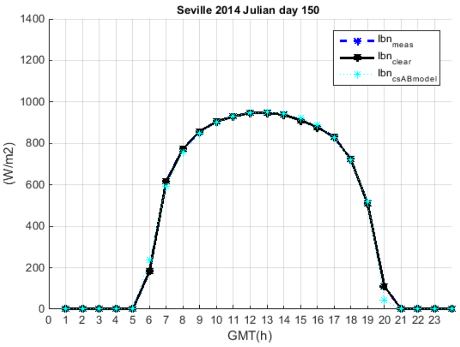
Seville 2014 Julian day 150
Ibn_{meas}
Ibn_{clear}
$Ibn_{csABmodel}$
(W/m2)
GMT(h)
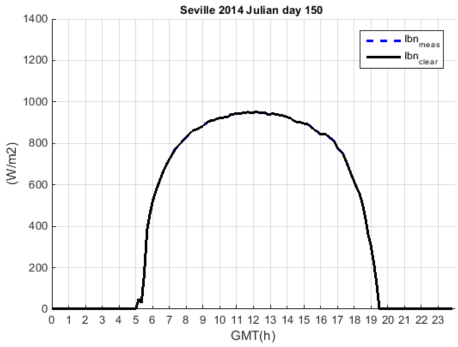
Seville 2014 Julian day 150
Ibn_{meas}
Ibn_{clear}
(W/m2)
GMT(h)
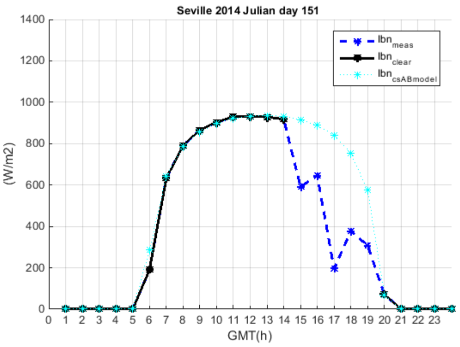
Seville 2014 Julian day 151
Ibn_{meas}
Ibn_{clear}
$Ibn_{csABmodel}$
(W/m2)
GMT(h)
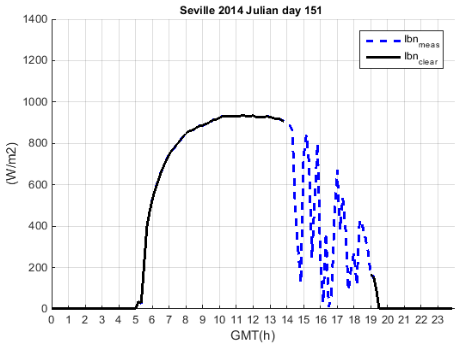
Seville 2014 Julian day 151
Ibn_{meas}
Ibn_{clear}
(W/m2)
GMT(h)

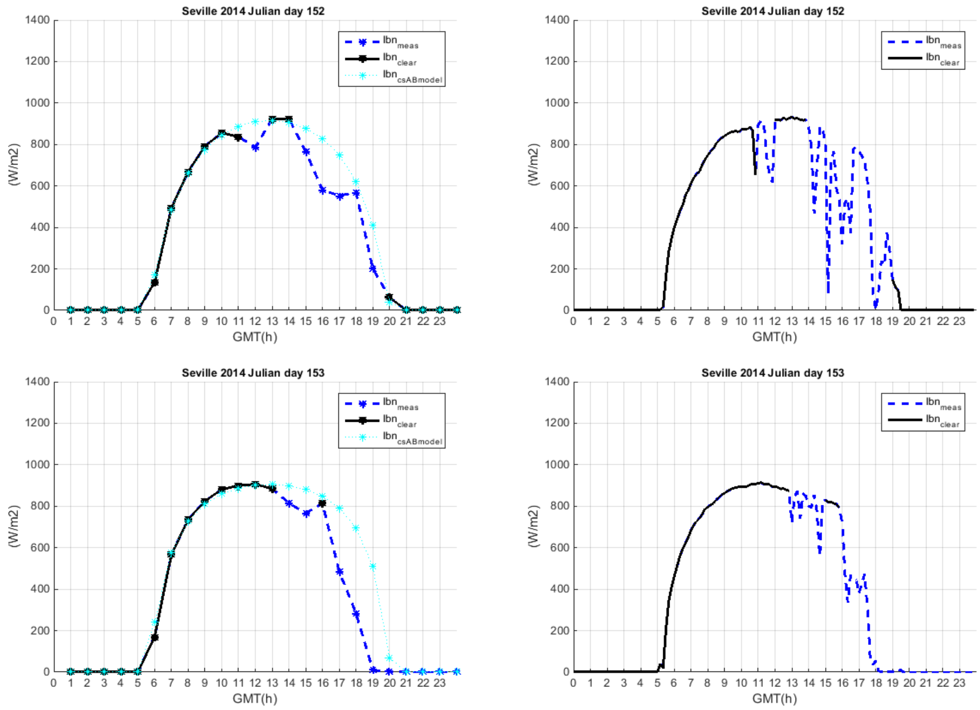

Fig 5. Illustrative daily examples.

In order to present a quantitative result, we have compared the results of the clear sky detection method presented here with the results of the algorithm proposed by Reno and Hansen [3]. The Reno and Hansen Algorithm uses 1-min means of GHI to detect periods with irradiance similar to the clear sky irradiance classifying each point of a 10-min moving window as clear or cloudy following five criteria:

- Mean value of GHI
- Maximum value of GHI
- Line length of irradiance vs. time curve
- Standard deviation of rate of change in GHI
- Maximum difference between changes in GHI and clear sky time series

The 1-minute resolution GHI data was obtained for the same location in Seville for 2014. The Reno and Hansen clear sky detection algorithm was applied to the GHI data to define each minute as clear or cloudy. In order to validate the hourly clear sky detection presented in this paper, the periods with irradiance similar to the clear sky irradiance are compared to the number of minutes in the hours identified as clear by the Reno and Hansen model. The percent of hours detected as clear with the methodology here proposed is shown in Fig 5. vs. the percent of minutes detected as clear with Reno and Hansen algorithm. Note that if the majority of minutes are clear (≥55% of the minutes), then the proposed algorithm demonstrates a high level of agreement, also defining the hour as clear.

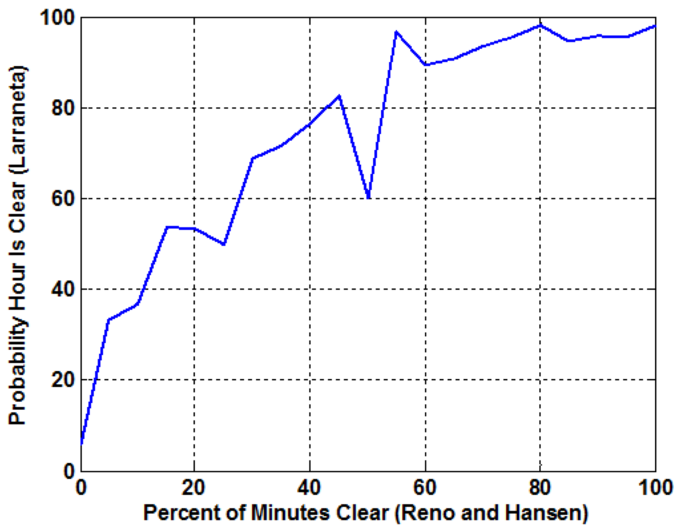

Fig 6. Percentage of 1-min daytime measurements identified as clear by Reno and Hansen versus the probability of an hour to be identified as clear by the methodology here presented.

Table 4 and presents the probability of an hour to be detected as clear depending on the number of minutes identified as clear in the corresponding hour by Reno and Hansen model. The analysis only takes into account complete daily hours.

Table 4. Percentage of identified clear hours versus number of clear minutes according to Reno and Hansen model.

	Reno and Hansen (clear minutes)						
	[60 - 50)	[50 - 40)	[40 - 30)	[30 - 20)	[20 - 10)	[10 - 0)	[0]
Larraneta (clear hours)	98%	94%	85%	72%	61%	41%	4%

It can be noticed that only in a few times one hour has been identified as clear with the methodology here presented when no minutes are defined as clear with Reno and Hansen methodology. On the opposite, for hours with many minutes identified as clear by Reno and Hansen, the hours are mostly identified as clear. The main discrepancy is observed when an intermediate number of minutes of one hour are identified as clear by Reno and Hansen model. In that case, in most of the times, the hours are identified as clear. Therefore, banks of fast clouds may not be detected with this methodology.

6 Conclusions

In this paper, we present a simple approach to identify periods with irradiance similar to the clear sky irradiance using only hourly DNI data as an input. The methodology relies on the proper fit of a clear sky model, which is iteratively adjusted. We presented results for tuning the A-B parameters of the fitted clear sky model to fourteen years of measured data in Seville. The novel clear sky detection algorithm presented in this paper identifies periods with irradiance similar to the clear sky irradiance by analyzing the mean, the slopes and the line length for both the measured and clear sky daily curves. The day is divided into three sections based on the solar elevation, and evaluation thresholds were established for each period and criteria. To address the performance of the methodology, we have compared the results with a recently published algorithm that uses one-minute measured GHI for the location of Seville in the year 2014. The proposed algorithm is shown to work accurately while not requiring high temporal resolution measurements. Identification of periods with clear sky equivalent DNI has wide application to design and operation of concentrated solar power systems.

References

[1] Younes, S., Muneer, T. Clear-sky classification procedures and models using a world-wide data-base. Appl. Energy, 84 (2007), pp. 623–645.

[2] Perez, R., Ineichen, P., Seals, R., Zelenka, A. Making full use of the clearness index for parameterizing hourly insolation conditions. Solar Energy, 45 (1990), pp. 111–114.

[3] Reno, M. J., Hansen, C.W. Identification of periods of clear sky irradiance in time series of GHI measurements Renewable Energy 90 (2016), pp. 520 – 531.

[4] Inman, R.H., Edson, J.G., Colmbra, C.F.M. Impact of local broadband turbidity estimation on forecasting of clear sky direct normal irradiance. Sol. Energy, 117 (2015), pp. 125–138.

[5] Nou, J., Chauvin, R., Traoré, A., Thil, S., Grieu, S. Atmospheric turbidity forecasting using side-by-side ANFIS. Energy Proc. 49 (2014), pp. 2387–2397. Proceedings of the Solar PACES 2013.

[6] Nou, J., Chauvin, R., Traoré, A., Thil, S., Grieu, S. A new approach to the real-time assessment of the clear-sky direct normal irradiance. Applied Mathematical Modelling 40 (2016), pp. 7245–7264.

[7] Larrañeta, M., Moreno, S., Silva, M.A., Lillo, I. An improved model for the synthetic generation of high temporal resolution direct normal irradiation time series. Solar Energy 122 (2015), pp. 517–528.

[8] Gueymard, C. A. Importance of atmospheric turbidity and associated uncertainties in solar radiation and luminous efficacy, modeling. Energy 30 (2005), pp. 1603–1621.

[9] Martínez-Chico, M., Batlles, F.J., Bosch J.L. Cloud classification in a Mediterranean location using radiation data and sky images. Energy 36 (2011), pp. 4055-4062.

[10] Markou, M.T., Bartzokas, A., Kambezidis, H.D. A new statistical methodology for classification of sky luminance distributions based on scan data. Atmospheric Research 86 (2007) 261-277.

[11] Hogan, R.J., Jakov, C., Illingworth, A.J. Comparison of ECMWF winter-season cloud fraction with radar-derived values. J. Appl. Meteorology 40 (2001) 513-525.

[12] Dupont, J.C., Haeffelin, M., Long, C.N. Evaluation of cloudless-sky periods detected by shortwave and longwave algorithms using Lidar measurements. Geophys. Res. Lett. 35 (2008).

[13] Orsini,A., Tomasi, C., Calzolari, F., Nardino, M., Cacciari, A., Georgiadis, T. Cloud cover classification through simultaneous ground-based measurements of solar and infrared radiation. Atmos. Res. 61 (2002) 251-275.

[14] Marty, C., Philipona, R. The Clear-Sky Index to separate clear-sky from cloudy sky situations in climate research. Geophys. Res. Lett. 27 (2000) 2649-2652.

[15] Behar, O., Khellaf, A., Mohammedi, K. Comparison of solar radiation models and their validation under Algerian climate – The case of direct irradiance. Energy Conversion and Management 98 (2015), pp. 236–251.

[16] Silva-Pérez, M.A. Estimación del recurso solar para sistemas termosolares de concentración. Doctoral thesis 2002. University of Seville.

[17] Kasten, F., Young A.T.Revised optical air mass tables and approximation formula. Applied Optics 28 (1989) 4735-4738.

[18] Kondratyev, K.Y. Radiation in the Atmosphere. Academic Press 1969, New York.

[19] Ohvril, H., Okulov, O., Teral, H. y Teral,K. The atmospheric integral transparency coefficient and the Forbes effect. Solar Energy 66 №4 (1999), pp. 305-317.

[20] Skartveit, A., Olseth, J.A. The probability density and autocorrelation of short-term global and beam irradiance. Solar Energy 49 (1192), pp. 477-487.